Theory of Operation of a 3-Port Y-Junction Ferrite Circulator*

E. N. SKOMAL†, SENIOR MEMBER, IRE

Summary—An analysis is made of the operation of a 3 port Y-junction ferrite circulator wherein it is assumed that the ferrite cylinder can support the propagation of a bound surface wave. The incident wave guided by the air-dielectric interface of the ferrite cylinder is taken to be linearly polarized parallel to the ferrite axis and after incidence on the cylinder is assumed to divide and propagate in opposite directions about the cylinder as two linearly polarized signals. By appropriate selection of ferrite cylinder diameter, permeability, magnetizing field and saturation magnetization, constructive and destructive interference of the RF components are shown to occur at the two output ports. The conditions for reinforcement and null at the outputs are discussed and compared with published experimental data. It is possible to predict the occurrence of ferrite circulator diplexing reported by Brown and Clark [9] although good quantitative comparison is lacking. The theoretical dependence of ferrite diameter upon free space wavelength is computed and compares satisfactorily with recorded experimental data. The experimental observations that greater circulator bandwidths are achievable when below resonance magnetizing fields are employed are shown to have a theoretical basis. In addition, interrelationships among the designed variables: saturation magnetization, applied magnetic field, ferrite resonance linewidth and circulator insertion loss are noted in the theoretical results.

Introduction

SUBSEQUENT to Chait and Curry's original announcement of a Y-junction ferrite circulator [1], various authors have reported experimental results on Y-junction ferrite circulator studies [2]–[9]. The reported work has spanned a range of frequencies from less than 150 Mc [5] to greater than 140,000 Mc [2]. Good results have been obtained over wide ranges of peak and average powers. At VHF, circulators have been operated at approximately 1 Mw peak and in excess of 2 kw average power [8]. Substantial efforts at miniaturization of low power circulators have been undertaken [6] which in general have been founded upon unique junction construction [5] and dielectric loading techniques [5], [6]. Mixed rare earth garnet materials have been successfully employed to achieve temperature stabilized performance by means of a reduction of the dependence of saturation magnetization on ambient temperature [6].

Theoretical interpretations of the circulation phenomenon in a symmetrical 3 port circulator have been published to supplement the experimental work. Auld considered a broad class of symmetrical microwave circulators and characterized their behavior in terms of appropriate scattering matrices, the coefficients of which were adjusted to reflect the inherent junction symmetries [10]. For a special member of the class, the 3 port Y circulator, he determined that two independent variables were sufficient to control circulator operation, these could be ferrite post diameter and magnetic field. Considerations of the 3 port junction symmetry and the implications of the device dependence upon ferrite diameter and magnetic field lead to a workable understanding of the circulator behavior.

In an analysis directed towards a physical interpretation of the Y-circulator operation, Bosma [11] investigated the cylindrically symmetric propagating modes which might be supported by a ferrite disk located in a strip transmission line 3 arm junction. The case of a ferrite disk with diameter comparable to the wavelength of the signal was studied. The appropriate group of cylindrical modes was found to possess no Z-axis variation and a zero of the azimuthal component of RF magnetic field at the disk circumference. From a consideration of the power flow conditions at the adjacent ports, Bosma concluded that circulator action could be controlled by either of two pairs of independent variables—1) ferrite post diameter and magnetic field (as noted by Auld), or 2) magnetic field and saturation magnetization.

The following analysis also treats the Y-junction circulator from a point of view selected to emphasize the physical behavior of the device. No stress is placed upon the type of transmission line which might be chosen to contain the ferrite material. Where it has been possible, comparisons with previous experimental observations have been made.

Analysis

Consider a cylinder of ferrite magnetized parallel to its axis as shown in Fig. 1. Incident on the wall of the ferrite cylinder is an RF magnetic field H_X perpendicular to the magnetizing field H_Z and tangent to the cylinder surface.

Relative to the point of incidence O are two additional points A and B separated from one another by equal central angles of 120° and together with O form a plane X-Y perpendicular to H_Z. The assumption is made that the incident RF field propagates as a surface wave tightly bound to the circumference of ferrite cylinder.

* Received September 28, 1962; revised manuscript received November 13, 1962.

† Motorola Solid State Systems Division, Phoenix, Ariz.

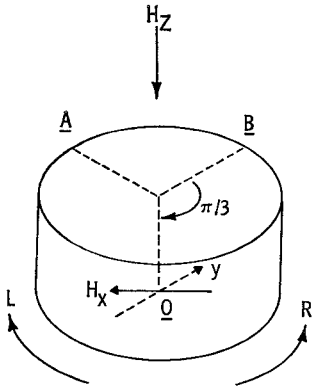

Fig. 1—Axially magnetized ferrite cylinder. A linearly polarized RF signal H_X is incident at point O with its magnetic vector tangent to the cylinder and parallel to the X axis.

In support of this assumption it should be noted that Seidel [12] and Bresler [13] have employed the concept of surface waves bound to and guided by the interface between a magnetized ferrite and its environment. Seidel interpreted the propagation of energy in a ferrite loaded transmission line of vanishingly small cross-section with the aid of a propagating surface wave bound to the ferrite interface adjacent to the waveguide wall.

The Lax-Button Thermodynamic Paradox [14] of a partially filled rectangular waveguide containing a full height ferrite slab was interpreted by Bresler in terms of two sets of propagating modes, the TE_{n0} waveguide modes identified by Lax, *et al.* [14], [15], and a set of TE_{n0} surface waves tightly bound to the ferrite-air interface. Bresler in addition related the surface waves of a partially filled ferrite loaded waveguide to the surface waves which predominate in a ferrite loaded parallel plate transmission line.

Clarricoats [16] has examined cases of guided wave propagation in the vicinity of dielectric rods for wide ranges of magnetic permeability μ and dielectric permittivity ϵ. His analyses have shown that bound surface waves at the air-dielectric interface can account for the transmission of energy in the two cases of 1) a dielectric rod located within a circular waveguide and 2) suspended in free space. Further, Clarricoats noted close correlation exists in the two cases between the dependence of the propagation constants upon frequency, rod diameter and $\mu\epsilon$. The percentage of total power carried by the surface wave in either case was calculated to increase with the ratio of rod diameter to free space wavelength and with $\mu\epsilon$.

Chandler [17] and Kiely [18] have recorded studies of surface wave propagation on a dielectric rod located in free space and have observed that surface waves will follow bends and curvatures of the rod transmission line. Radiation losses associated with propagation around a bend were noted to increase as the radius of curvature decreased, for a constant rod diameter, and also to increase as rod diameter decreased, for a constant radius of curvature.

In the present instance of an RF signal incident upon the lateral surface of the ferrite ϵ cylinder, the radius of curvature of the cylinder, the frequency, the dielectric constant of the ferrite and the magnetic permeability μ can be expected to determine the extent of coupling of the surface wave to the cylinder, thus the radiation loss, and, therefore, in part, the insertion loss and isolation of the circulator.

It is further assumed that after incidence the surface wave divides equally and propagates circumferentially from point O towards both the left and right. The component L (propagating to the left) and component R (propagating to the right) are considered to be linearly polarized and, therefore, can be individually resolved into circularly polarized components rotating in clockwise and counter clockwise directions relative to the magnetizing field H_Z. For arbitrary values of $H_Z > 0$ the propagation velocities of the circularly polarized fields will differ. Accordingly, the circularly polarized components of the magnetic field incident at O will arrive at points A and B and produce resultant RF magnetic field vectors, lying in the X-Y plane, which are rotated away from the X axis. Upon the selection of a biasing magnetic field H_Z which yields a higher propagation velocity for the positively circularly polarized component of the RF magnetic field than for the negatively circularly component, the resultant magnetic field at A or B will be rotated towards the positive Y axis by an angle θ. The static magnetic field H_Z, the saturation magnetization of the cylinder $4\pi M_S$ and the diameter of the cylinder D can be chosen to cause the circularly polarized components originating at O to arrive at points A and B with their linearly polarized resultants rotated clockwise 30°. The significance of the value of $\theta = 30°$ will be stressed in the following paragraphs.

The condition for the occurrence of a rotation $\theta = 30°$ of the linearly polarized resultants arriving at points A and B is

$$\frac{\pi D}{6}(\beta_- - \beta_+) = \frac{\pi}{6} \quad \text{or} \quad D(\beta_- - \beta_+) = 1 \qquad (1)$$

where D is the cylinder diameter and β_- and β_+ are the propagation constants for the positively and negatively circularly polarized RF magnetic fields. It is assumed that the attenuation constants for the circularly polarized components are equal thereby preserving the linear polarization. It is generally possible to produce the condition wherein the negatively circularly polarized signal is propagated at a higher velocity than the positively polarized component. When this occurs the linearly polarized resultant is rotated towards the negative Y axis as the surface wave propagates away from O. For this case the positions of β_+ and β_- in (1) are interchanged.

If the diameter of the ferrite cylinder, its saturation magnetization, the magnetizing field and frequency are selected to produce the condition where the circumferen-

tial separation between adjacent pairs of points O, A and B is one wavelength for the surface wave, the left and right hand components of the incident signal will circulate about the circumference repeatedly arriving in phase at each point, O, A and B, with, however, differing orientations of the magnetic vector. After the fourth circulation, assuming (1) has been satisfied, the orientation of the linearly polarized resultants at points O, A and B will begin to repeat in value.

This process is pictured in Fig. 2(a). The RF field H_X lying in the X-Y plane is linearly polarized tangentially to the ferrite cylinder when incident at point O. The linearly polarized surface waves propagating to the left and right are indicated by L and R. At points O, A and B are shown the orientations of L and R at each arrival. The number associated with each arrow indicates the index of the circulation, the first arrival of wave L at A results in a polarization orientation perpendicular to the tangent while the first arrival of wave R at A yields a polarization rotated 30° clockwise relative to the diameter. First circulation arrivals at O for waves L and R are normal to the tangent at O. Dissipative and radiative losses in the system will gradually diminish the surface wave amplitudes. If the losses are appreciable, only the first circulation will be significant, as indicated in Fig. 2(b), where only the first circulation and the incident field vector H_X are shown.

If at points A and B direction sensitive detection probes are positioned in a fashion to couple to the tangential component of the surface wave, the transmitted signals P_A and P_B detected at A and B will be

at A

$$P_A = K^2\left(\frac{H_x^2}{4\sqrt{2}}\right) = \frac{P_{\text{in}}}{32} = 0.03P_{\text{in}}$$

from surface wave R;

at B

$$P_B = K^2\left[\left(\frac{H_x}{\sqrt{2}}\right)^2 + \left(\frac{H_x\sqrt{3}}{2\sqrt{2}}\right)^2\right]$$

$$= \tfrac{7}{8}K^2H_x^2 = 0.88P_{\text{in}}$$

from surface waves L and R,

where $P_{\text{in}} = K^2H_x^2$ and K^2 is a constant of the transmission system.

At point O no signal will be coupled out after the first circulation of waves L and R. In practice the input power not represented by the sum of P_A and P_B above can be coupled to port B by introducing reactances at points A and B.

One sees that the majority of the input power is coupled to B, a small portion to A and none back to O provided (1) is satisfied and that the circumferential

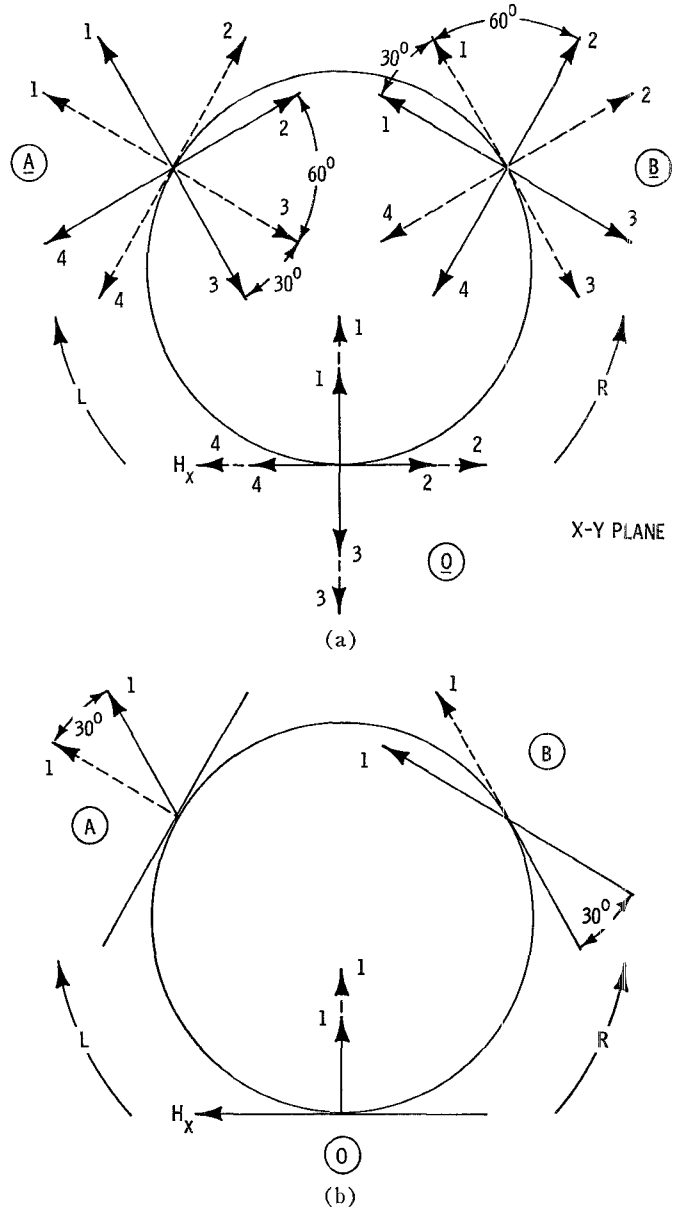

Fig. 2—(a) Orientations of the RF magnetic field vectors at points O, A and B for four complete rotations of the surface waves: *left*—dotted arrows, *right*—solid arrows. The incident field H_X and the fourth rotation components at point O are colinear. Rotation numbers are entered beside the arrows. (b) The orientation of the RF magnetic field vectors for one complete rotation of surface waves L and R.

distance between adjacent points is equal to λ_s, the surface wave wavelength. This condition is expressible as

$$\beta_s \cdot \frac{\pi D}{3} = 2\pi$$

$$\beta_s D = 6 \qquad (2)$$

where β_s is the propagation constant for the surface wave which is assumed to remain linearly polarized during circulation.

Considering now the propagation constants β_+ and β_- from (1) and β_s from (2), approximate expressions for these quantities can be written for an RF field propagating in a ferrite ellipsoid with cylindrical symmetry,

magnetized by a field H_A perpendicular both to the direction of wave propagation and to the direction of polarization of the incident RF magnetic field.

The isotropic propagation constants, in the absence of losses, are

$$\beta_s = \frac{2\pi\sqrt{\epsilon}}{\lambda_0}\sqrt{\frac{2\mu_+\mu_-}{\mu_+ + \mu_-}}$$

$$\beta_- = \frac{2\pi\sqrt{\epsilon}}{\lambda_0}\sqrt{\mu_-}$$

$$\beta_+ = \frac{2\pi\sqrt{\epsilon}}{\lambda_0}\sqrt{\mu_+}$$

$$\mu_\pm = 1 \mp \frac{\omega_m}{\omega \mp \omega_0} \qquad \text{Circular permeabilities}$$

$$\frac{\omega_m}{\gamma} = 4\pi M_s \qquad \text{Saturation magnetization}$$

$$\omega_0 = \gamma H_{\text{eff}}$$

$$H_{\text{eff}}^2 = [H_A + (N_X - N_Z)M_s][H_A + (N_Y - N_Z)M_s].$$

N_X, N_Y, Z_Z are the static demagnetizing factors for an ellipsoid, γ is the gyromagnetic ratio, ω the angular frequency, H_{eff} is the effective resonance magnetic field and H_A the external applied magnetic field.

Solving (1) and (2) simultaneously one obtains

$$\beta_s = 6(\beta_- - \beta_+) \qquad \text{for } \beta_- > \beta_+ \tag{3a}$$

or

$$\beta_s = 6(\beta_+ - \beta_-) \qquad \text{for } \beta_+ > \beta_-. \tag{3b}$$

In terms of the positive and negative circular permeabilities (3) can be written as

$$\left(\frac{\mu_+}{\mu_-}\right)^4 - b\left(\frac{\mu_+}{\mu_-}\right)^3 + c\left(\frac{\mu_+}{\mu_-}\right)^2 - d\left(\frac{\mu_+}{\mu_-}\right) + 1 = 0 \tag{4}$$

where

$$b = d = \left[\frac{4}{R^2}\right] = \frac{1}{9}$$

[for $R=6$ where R is the ratio of the right-hand sides of (2) and (1)] and

$$c = \left[\frac{4}{R^4} - \frac{8}{R^2} - 2\right] = -\frac{719}{324}.$$

The real positive roots of (4) are

$$\frac{\mu_+}{\mu_-} = 0.72 \quad \text{and} \quad 1.4. \tag{5a}$$

For the case where $\mu_- > \mu_+$, considering the symmetry of (3), the real positive roots are seen to be

$$\frac{\mu_-}{\mu_+} = 0.72 \quad \text{and} \quad 1.4. \tag{5b}$$

The root 1.4 yields a negative value for D when substituted into (1) and must be discarded. Only the root 0.72 represents a physically realizable condition. The corresponding values of D, for the cases where H_{eff} is 1) less than and 2) greater than the field for resonance, are

$$D_1 = \frac{\lambda_0}{2\pi\sqrt{\epsilon\mu_-}} = \frac{6.6\lambda_0}{2\pi\sqrt{\epsilon\mu_-}} = \frac{1.0\lambda_0}{\sqrt{\epsilon\mu_-}}$$

effective magnetic field below resonance.

and

$$D_2 = \frac{1.0\lambda_0}{\sqrt{\epsilon\mu_+}} \qquad \text{effective magnetic field above resonance.}$$

When the effective magnetic field is greater than resonance value, $\mu_+ > \mu_-$ and D_2 is less than D_1, their ratio being

$$\frac{D_2}{D_1} = \sqrt{\frac{\mu_-}{\mu_+}} = \sqrt{0.72} = 0.85.$$

Thus, in device design some decrease in size of the ferrite cylinder is achievable by using an above resonance magnetizing field.

When the solution $\mu_+/\mu_- = 0.72$ is expressed in terms of ω_m, ω_0 and ω, the resulting equation

$$\omega_0^2 + \omega_m\omega_0 + 6.14\omega\omega_m - \omega^2 = 0 \tag{6}$$

places a restraint upon the range of the possible values of ω_m.

For several cylindrically symmetric ferrite configurations an upper limit on ω_m is imposed beyond which $H_A = 0$.

For the sample geometrics of a sphere, rod and disk the values of ω_m for which $H_A = 0$ are shown in Table I.

TABLE I

Sample Shape	Static Demagnetizing Factors	Dependence of ω_m on ω for $H_A = 0$	Value of $4\pi M_S$ for $H = 0$; $f = 7.4$ Gc
Sphere	$N_X = N_Y = N_Z = \frac{4\pi}{3}$	$\omega_m = \frac{\omega}{6.14}$	433 oersteds
Rod	$N_X = N_Y = 2\pi \quad N_Z = 0$	$\omega_m = \frac{\omega}{6.2}$	429 oersteds
Disk	$N_X = N_Y = 0; \quad N_Z = 4\pi$	$\omega_m = \frac{\omega}{6.14}$	433 oersteds

Comparison of the Computations with Various Experimental Data

Brown and Clark [9] have measured the dependence of the applied magnetic field H_A upon $4\pi M_S$ for the condition of optimum operation of a 3 port circulator. Two conditions were studied: 1) H_A above and 2) H_A below resonance. The measurements for H_A below resonance were performed at a frequency of 7.4 Gc and reveal

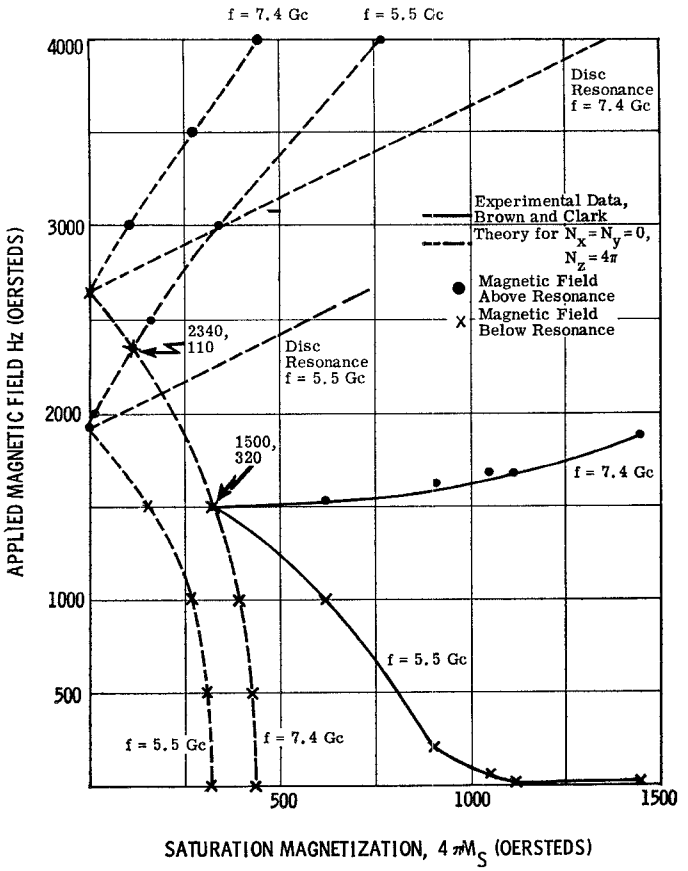

Fig. 3—Applied magnetic field vs sample saturation magnetization for optimum circulator operation.

that for $H_A=0$; $4\pi M_S \simeq 1100$ oersteds. (See Fig. 3.) The values of $4\pi M_S$ corresponding to $H_A=0$ computed for the three sample geometrics at $f=7.4$ Gc are shown in the last column of Table I.

For the condition that H_A is above resonance the solution to (4) is $\mu_-/\mu_+=0.72$ which when expressed in terms of ω_m, ω_0 and ω reveals that $H_A>0$ for all values of $4\pi M_S$.

Brown and Clark have shown that for the proper choice of ω_m, H_A and ω, a 3 port circulator will diplex two signals which have been injected into one port presenting them separately at the alternate output ports. Referring to Fig. 1, when two signals incident at O are so chosen in frequency that the effective magnetic field H_{eff} is

$$\frac{f_2}{\gamma} < H_{\text{eff}} < \frac{f_1}{\gamma},$$

signal f_1 will emerge only at A and signal f_2 only at B.

The occurrence of this effect can be predicted by equating the solutions of (4) for the two cases where

$$\mu_+ > \mu_- \text{ and } \mu_- > \mu_+$$

that is,

$$\frac{\mu_+}{\mu_-} = \frac{\mu_-}{\mu_+} = 0.72$$

which leads to the expression

$$H_A^2 - \frac{H_A}{6.14\gamma}(f_1 - f_2) - \frac{f_1 f_2}{\gamma^2} = 0 \qquad (7)$$

for a disk $N_X = N_Y = 0$

$$N_Z = 4\pi.$$

The resulting value of $4\pi M_S$ can be obtained by substituting the solution for H_A from (7) into (6) which has been solved for $4\pi M_S$:

$$4\pi M_S = \frac{\left(\frac{f_1}{\gamma}\right)^2 - H_A^2}{6.14\left(\frac{f_1}{\gamma}\right) - H_A}; \qquad \begin{aligned} &H_{\text{eff}} < \frac{f_1}{\gamma} \\ &N_X = N_Y = 0 \\ &N_Z = 4\pi. \end{aligned} \qquad (8)$$

For $f_1=7.4$ Gc and $f_2=5.5$ Gc, (7) and (8) yield $H_A=2340$ oersteds and $4\pi M_S=110$ oersteds which must be compared with Brown and Clark values of $H_A=1500$ oersteds and $4\pi M_S=320$ oersteds respectively.

The value of $H_Z=H_A$ from (8) is plotted in Fig. 3 vs $4\pi M_S$. Also included in Fig. 3 is a plot of H_Z vs $4\pi M_S$ for the condition of H_{eff} greater than resonance obtained from the expression

$$4\pi M_S = \frac{H_A^2 - \left(\frac{f_2}{\gamma}\right)^2}{H_A + 6.14\left(\frac{f_2}{\gamma}\right)} \qquad \begin{aligned} &N_X = N_Y = 0 \\ &N_Z = 4\pi. \end{aligned} \qquad (9)$$

Included in Fig. 3 are the data of Brown and Clark. The similarity of trends is apparent however the quantitative agreement is not close.

The discrepancy between the computed curves and the Brown and Clark data is of such a nature that were a smaller value than $\theta=30°$ chosen for the total rotation of the circularly polarized components between adjacent ports, the experimental and theoretical agreement would be improved. In fact, for $\theta \simeq 15°$ rather good agreement can be obtained. To make this assumption would introduce a new problem, *i.e.*, the relative isolation between ports A and B would sharply deteriorate, although it might then be argued that by the introduction of additional reactance at ports A and B the original isolation could be restored. Although this can be accomplished empirically, there is no evident way to include the effects of such adjustments in these computations.

A less significant factor contributing to the discrepancy is the exact value of the static demagnetizing factors to be used in comparing these computations with the Brown and Clark data. It was presumed herein that the ferrite geometry was a thin flat disk.

The computed dependence of ferrite disk diameter upon λ_0

$$D_{1,2} = \frac{1.0\lambda_0}{\sqrt{\epsilon\mu_\mp}}$$

can be compared with the VHF/UHF data of Buehler [5] *et al.*, Curves I and III, Fig. 3, where ferrite disk diameter is plotted vs frequency for two center conductor configurations. A nearly linear dependence of disk diameter upon free space wavelength is revealed by Buehler's data. Buehler's Curve III for a Y-junction containing a dielectric matching ring surrounding the ferrite displays a dependence upon wavelength of the form $D=A\lambda_0-B/\lambda_0$ which is probably attributable to the occurrence of dielectric dispersion.

Experimental data presented by Bosma [11] for the variation of ferrite disk diameter with frequency in the range of 500 Mc to 3 Gc also reveals a linear dependence of ferrite diameter upon wavelength as predicted by the theory.

A quantitative comparison of the experimental data of Buehler and Bosma with the expressions for D_1 and D_2 is not possible since in each instance insufficient experimental information is presented to permit the calculation of $\mu_\pm$.

Circulator Design Comments

It is of interest to determine the dependence of optimum circulator operation upon frequency for the conditions of H_{eff} above and below resonance.

The conditions for circulator operation are given in (5a) and (5b) which written in terms of the quantities ω, ω_0 and ω_m are

$$F_{\text{below}}(\omega) = \omega_0^2 + \omega_0\omega_m + 6.14\omega\omega_m - \omega^2 = 0$$

$$F_{\text{above}}(\omega) = \omega_0^2 + \omega_0\omega_m - 6.14\omega\omega_m - \omega^2 = 0.$$

Differentiating with respect to ω gives

$$\frac{dF_{\text{below}}(\omega)}{d\omega} = 6.14\omega_m - 2\omega$$

$$\frac{dF_{\text{above}}(\omega)}{d\omega} = -6.14\omega_m - 2\omega$$

$$\therefore \left|\frac{dF_{\text{above}}(\omega)}{d\omega}\right| > \left|\frac{dF_{\text{below}}(\omega)}{d\omega}\right|.$$

These results are in accord with the experimental observation that maximum circulator bandwidths are achieved for circulators operating with below resonance magnetizing fields.

Also plotted in Fig. 3 is Kittel's resonance equation for a disk, $H_A=f/\gamma+4\pi M_S$ computed for $f=5.5$ and 7.4 Gc. Inspection of the computed curves (Fig. 3) for a disk configuration reveals several points of design interest:

1) For below resonance operation at a fixed frequency and constant $4\pi M_S$, a ferrite with a broader linewidth, ΔH, can be employed than is possible in above resonance operation without degrading circulator insertion loss.
2) For optimum circulator operation above resonance, at a fixed frequency, the optimum applied magnetic field H_Z increases more rapidly with $4\pi M_S$ than does the applied field required to resonate the disk.
3) For optimum circulator operation below resonance, at a fixed frequency, the optimum applied field H_Z decreases as $4\pi M_S$ increases.

References

[1] H. N. Chait and T. R. Curry, "Y-circulator," *J. Appl. Phys.*, vol. 30, pp. 152–153S; April, 1959.
[2] J. B. Thaxter and G. S. Heller, "Circulators at 70 and 140 kMc," Proc. IRE, vol. 48, p. 110; January, 1960.
[3] U. Milano, J. H. Saunders, and L. Davis, Jr., "A Y-junction strip-line circulator," IRE Trans. on Microwave Theory and Techniques, vol. MTT-8, pp. 346–351; May, 1960.
[4] S. Yoshida, "Strip-line Y-circulator," Proc. IRE, vol. 48, pp. 1337–1338; July, 1960.
[5] G. V. Buehler and A. F. Eikenberg, "Strip-line Y-circulators for the 100- to 400-Mc region," Proc. IRE, vol. 2, pp. 518–519; February, 1961.
[6] J. Clark and J. Brown, "Miniaturized, temperature stable, coaxial Y-junction circulators," IRE Trans. on Microwave Theory and Techniques, vol. MTT-9, pp. 267–269; May, 1961.
[7] J. Clark, "Perturbation techniques for miniaturized coaxial Y-junction circulators," *J. Appl. Phys.*, vol. 32, pp. 323–324; March, 1961.
[8] G. V. Buehler and A. F. Eikenberg, "A VHF high-power Y-circulator," IRE Trans. on Microwave Theory and Techniques, vol. MTT-9, pp. 569–570; November, 1961.
[9] J. Brown and J. Clark, "A unique solid-state diplexer," IRE Trans. on Microwave Theory and Techniques, vol. MTT-10, p. 298; July, 1962.
[10] B. A. Auld, "The synthesis of symmetrical waveguide circulators," IRE Trans. on Microwave Theory and Techniques, vol. MTT-7, pp. 238–246; April, 1959.
[11] H. Bosma, "On the principle of strip-line circulation," *Proc. IEE (London)*, vol. 109, pt. B (suppl.), pp. 137–146; January, 1962.
[12] H. Seidel, "Anomalous propagation in a ferrite-loaded waveguide," Proc. IRE, vol. 44, pp. 1410–1414; October, 1956.
[13] A. D. Bresler, "On the TE_{n0} modes of a ferrite slab loaded rectangular waveguide and the associated thermodynamic paradox," IRE Trans. on Microwave Theory and Techniques, vol. MTT-8, pp. 81–95; January, 1960.
[14] B. Lax and K. J. Button, "Theory of new ferrite modes in rectangular waveguide," *J. Appl. Phys.*, vol. 26, pp. 1184–1185; September, 1955.
[15] B. Lax, K. J. Button, and L. M. Roth, "Ferrite phase shifters in rectangular waveguide," *J. Appl. Phys.*, vol. 25, pp. 1413–1421; November, 1954.
[16] P. J. B. Clarricoats, "Propagation along unbounded and bounded dielectric rods," *Proc. IEE*, Mono. 409E, pp. 170–186; October, 1960.
[17] C. H. Chandler, "An investigation of a dielectric rod as a waveguide," *J. Appl. Phys.*, vol. 20, pp. 1185–1192; December, 1949.
[18] D. G. Kiely, "Progress in Dielectrics," vol. 3, pp. 1–47; 1961.